Visualization and Measurement of High-Temperature and High-Speed Gas-Solid Two-Phase Jet

M. Yokohama[1], H. Ishikawa[2] and M. Suzuki[3]*

1: Dept. of Mechanical Engineering, Graduate School, Tokyo University of Science, Japan
2: Dept. of Mechanical Engineering, Tokyo University of Science, Japan
3: Aviation Technology Directorate, Japan Aerospace Exploration Agency, Japan

* Correspondent author: suzuki.masaya@jaxa.jp

Abstract

The gas-solid two-phase flow at high temperatures and high velocity is important for industrial technologies such as thermal spraying. We analyzed gas-solid two-phase flow at high temperatures and high velocity using PIV and probes to clarify the behavior of the flow. In the flow, the speed of gas and solid particles decreased as they travel downstream. The gas and particles have a velocity component that moves away from the center of the flow. Comparing the gas and solid particles, the speed of gas is higher in upstream, but the speed of solid particles is higher in downstream. In conditions that exceed the speed of sound, shock diamond occurred with the gas, but not with the solid particles. In the flow, the static temperature and the velocity of solid particles are proportional.

Keyword: *Jet Engine, Jet Flow, Erosion, Deposition, Particle Image Velocimetry*

1. Introduction

Erosion and deposition occur in aviation jet engines when they inhale fine particles such as sand, volcanic ash, and yellow sand suspended in the atmosphere during operation. These phenomena can lead to a decline in engine performance and lifetime and even cause serious accidents. Therefore, it is necessary to understand erosion and deposition mechanisms to improve the erosion and deposition resistance of the engine. Balan and Tabakoff [1] measured the degree of erosion by impinging quartz particles on two-dimensional accelerating/decelerating cascades of airfoils and a single-stage axial flow compressor to investigate the performance degradation caused by the erosion. The results revealed that erosion significantly reduces the aerodynamic performance of the cascade.

To understand the mechanisms of erosion and deposition in jet engines, an efficient way is experiments in which a high-temperature and high-speed gas-solid two-phase flow impinges on a specimen. However, as a preliminary step, it is necessary to understand the behavior of the particle-laden flow. Understanding the flow behavior can also be applied to industrial technologies such as thermal spraying. Kuroda et al. [2] calculated the velocity of the gas and the particles ejected from a warm spray barrel. The results showed that the gas has a greater velocity than the particles, but after a certain distance from the barrel, the gas has a smaller velocity than the particles.

In this study, we clarified the flow behaviors of the gas-solid two-phase jet in high-temperature and high-speed conditions using a high-temperature difference burner — material and coating test apparatus [3] and measured the flow using particle image velocimetry (PIV) and thermocouple and pressure probes.

2. Experimental Apparatus

2.1 Measurement of the Flow by PIV

Fig. 1 shows a schematic of this experiment. In this experiment, we clarified the flow behaviours of the gas-solid two-phase jet in high-temperature and high-speed conditions using a high-temperature difference burner — material and coating test apparatus and measured the flow using PIV. This test apparatus generates high-temperature and high-speed combustion gas using a HVAF (High-Velocity Air Fuel) burner that uses kerosene

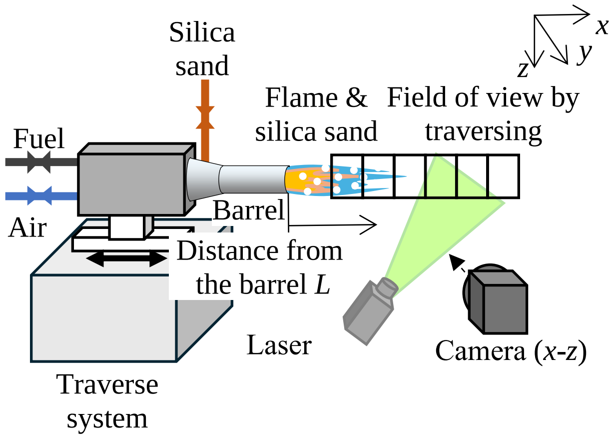

Fig. 1 Experimental setup for measurement of gas-solid two-phase flow by PIV

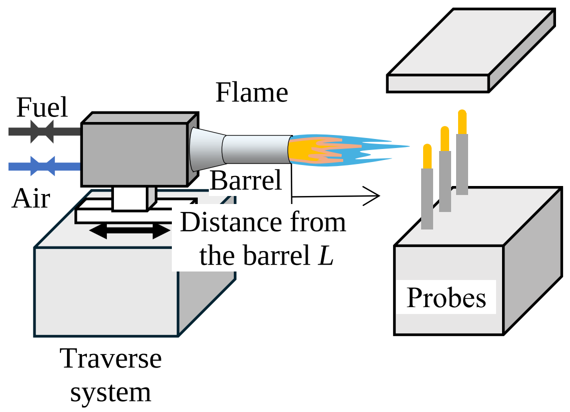

Fig. 2 Experimental setup for measurement of gas flow by temperature and pressure probes

as the fuel and compressed air as the oxidizing agent. Solid particles are injected downstream of the burner combustion chamber and accelerated within the barrel. To measure airflow, porous silica particles with an average diameter of 1 μm were used as tracer particles. For the particulate flow measurements, silica with a diameter of 27 μm to 31 μm was used since silica is a typical sand component suspending the atmosphere, and the size is important for the erosion of hot sections in jet engines.

Stokes numbers (S_t [-]) indicate followability of the particle to the flow. At a distance of 100 mm and a velocity of 600 m/s, the stokes numbers of the tracer particles S_t = 0.0476 and of the solid particles S_t = 40.0.

The combustion conditions are constant at an air-fuel ratio of 22, and air flow rate Q_{air} and fuel flow rate Q_{fuelr} are changed. The experiment was conducted under the following three conditions, Q_{air} =32 g/s- Q_{fuel} = 1.45g/s, Q_{air} = 40 g/s - Q_{fuel} =1.45 g/s, Q_{air} = 48 g/s - Q_{fuel} =2.18 g/s.

Tracer particles and solid particles were visualized by irradiating the *x*-*z* cross-section with a double-pulsed laser (Nano S 50-20PIV, repetition frequency 0~20 Hz, wavelength 532 nm, pulse energy 50 mJ), and images were taken using a double-shutter camera (pco.1600, resolution 1 600 × 1 200 pixels, frame rate 0~30 fps, minimum straddling time: 120 ns). By moving the burner with a traverse device, the distance from the burner *L* [mm] was taken in the range of *L* = 14 mm to *L* = 359 mm for the gas flow and *L* = 5 mm to *L* = 351 mm for the solid particle flow.

2.2 Measurement of the Flow by Probes

In this experiment, we measured the total pressure P_t [Pa], static pressure P_s [Pa] and total temperature T_t [K] of the combustion gas flow by a temperature probe and pressure probes. Fig. 2 shows a schematic of this experiment. The velocity V [m/s] and static temperature T_s [K] of the flame are calculated from the measured total pressure, static pressure, and total temperature. The equations required for calculation are shown in equation (1) ~ (5) below. In these equations, we define specific heat ratio γ = 1.4 [-], Mach number M [-], density of air ρ [kg/m^3], gas constant R =287 [J/(kg·K)], and speed of sound a [m/s], respectively.

$$T_s = \frac{T_t}{\left(\frac{P_t}{P_s}\right)^{\frac{\gamma-1}{\gamma}}} \tag{1}$$

$$M = \sqrt{\frac{2}{\gamma-1}\left(\frac{T_t}{T_s}-1\right)} \tag{2}$$

$$\rho = \frac{P_s}{RT_s} \tag{3}$$

$$a = \sqrt{\gamma\frac{P_s}{\rho}} \tag{4}$$

$$V = Ma \tag{5}$$

3. Experimental Results and Discussion

3.1 Visualization of Gas-Solid Two-Phase Jet by PIV

Fig. 3 shows the visualization results of the gas flow and the solid particle flow at each combustion condition measured using PIV. The left figures show the velocity component in the *x* direction *u* [m/s], and the right figures show the velocity component in the *z* direction *w* [m/s]. These figures were made by combining the results of six series of pictures measured at each traversing position.

The upper left parts of the figures are masked in black, which are the part that are blocked by the barrel and are not irradiated by the laser beam. In addition, since the flame is not diffused upstream, the tracer particles and the solid particles do not enter at the point away from the center of the flame, and there are many errors.

When burned at the same air-fuel ratio, the larger air flow rate and fuel flow rate, the larger velocity in the *x* direction of the gas flow and solid particle flow. This is because the velocity also increased due to the increase in the flow rate. The velocity in the *x* direction of both gas and solid particles tends to decrease as the distance from the barrel L increases. This is because as the distance increases, the kinetic energy attenuates due to the diffusion and mixing with the surrounding low-speed air. Comparing the gas and solid particles, the velocity in the *x* direction of solid particles is greater.

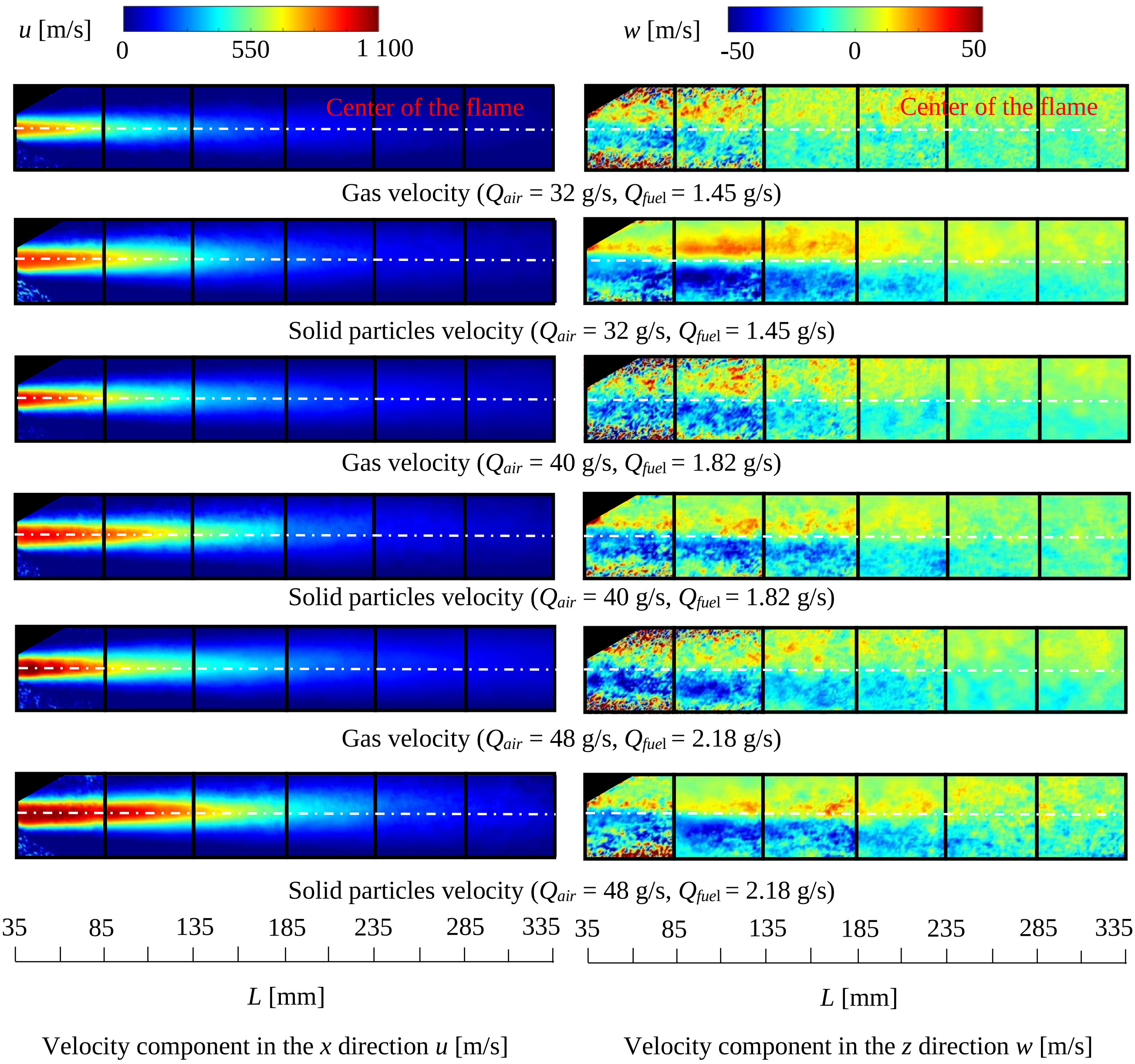

Fig.3 Visualization of gas-solid two-phase jet by PIV

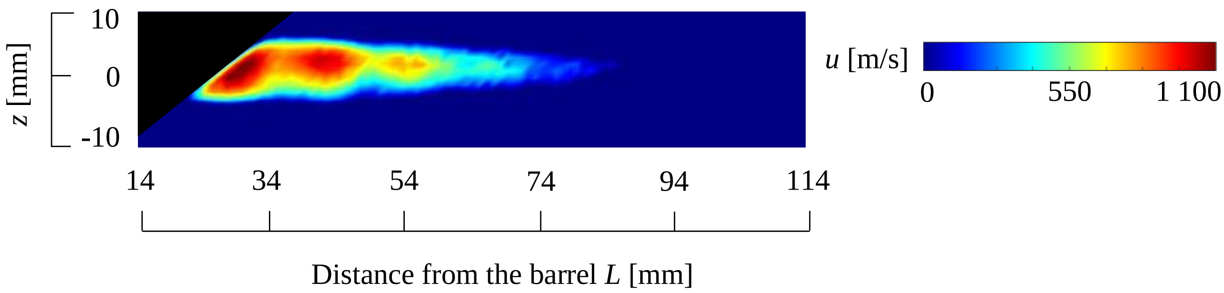

Fig.4 Diamond shock at high-velocity condition (Q_{air} = 48 g/s, Q_{fuel} = 2.18 g/s)

Next, the velocity in the direction *z* of both gas and solid particles tends to close to 0 m/s at the center of the flame, and to leave away from the flame center. Comparing the gas and solid particles, there were no significant difference due to the difference in combustion conditions.

Fig. 4 shows the visualization results of the gas flow near the barrel under the combustion conditions of Q_{air} = 48 g/s and Q_{fuel} = 2.18 g/s. In this figure, the color map is adjusted from the velocity distribution in Figure 3 to make it easier to see the trend. The upper left parts of the figure is masked in black, which is the part that is blocked by the barrel and is not irradiated by the laser beam. There are places where the speed is faster than the surroundings. This is a phenomenon called shock diamond[4], in which a shock wave is generated when the gas flow becomes supersonic, forming the shape of a diamond. Under other combustion conditions, in the case of gas flow, there is no clear difference from the surrounding area as the flow rate decreases, and this could not be confirmed in the flow of solid particles. This is due to the fact that the smaller the flow rate, the smaller the velocity, making it difficult for shock waves to be generated, and the fact that solid particles have a large Stoke number and therefore have low followability to the gas flow.

3.2 Comparison of Velocity obtained by PIV and Probes

Fig. 5 shows the velocity of the gas flow and solid particles in the center of the flame measured by PIV and the velocity of the gas flow calculated from the total pressure, static pressure, and total temperature measured by the probes. The horizontal axis the distance from the barrel *L* and the vertical axis are velocity *V*, and the blue solid square symbols are the gas flow velocity measured by PIV, the pink cross symbols are the solid particle flow velocity measured by PIV, and the blue hollow square symbols are the gas flow velocity calculated using equations (1) ~ (5) from the measurement results of the probes. The results of the measurement of the PIV and the probes were in good agreement with the gas flow velocity under the all combustion conditions, indicating the validity of the measurement results of both methods. Comparing the gas flow velocity due to PIV and the solid particle flow velocity, the gas flow velocity is larger near the barrel and the velocity is equal around L=50 mm, and the velocity of the solid particle increases as the distance increases, and the velocity is equal again near L=250 mm under all combustion conditions. This is because the Stokes number is so small that, the gas flow become faster near the barrel. However the solid particles have a large mass, the kinetic energy is large, and the solid particles are less affected by the energy decay caused by the surrounding air. The solid particles are faster in the middle part, and eventually the velocity decreases due to the influence of air resistance due to the size of the particles, and the speed becomes similar to that of the gas flow.

3.3 Velocity and Static Temperature of gas flow

Fig. 6 shows a graph comparing the static temperature of the flame calculated from the probes measurement at the same distance and the approximate value from the solid particle velocity measured by PIV. In this graph, the horizontal axis the velocity *V* and the vertical axis are Static temperature T_s, and the pink square symbols are Q_{air} = 32 g/s, Q_{fuel} = 1.45 g/s, the blue square symbols are Q_{air} = 40 g/s, Q_{fuel} = 1.82 g/s, and the green

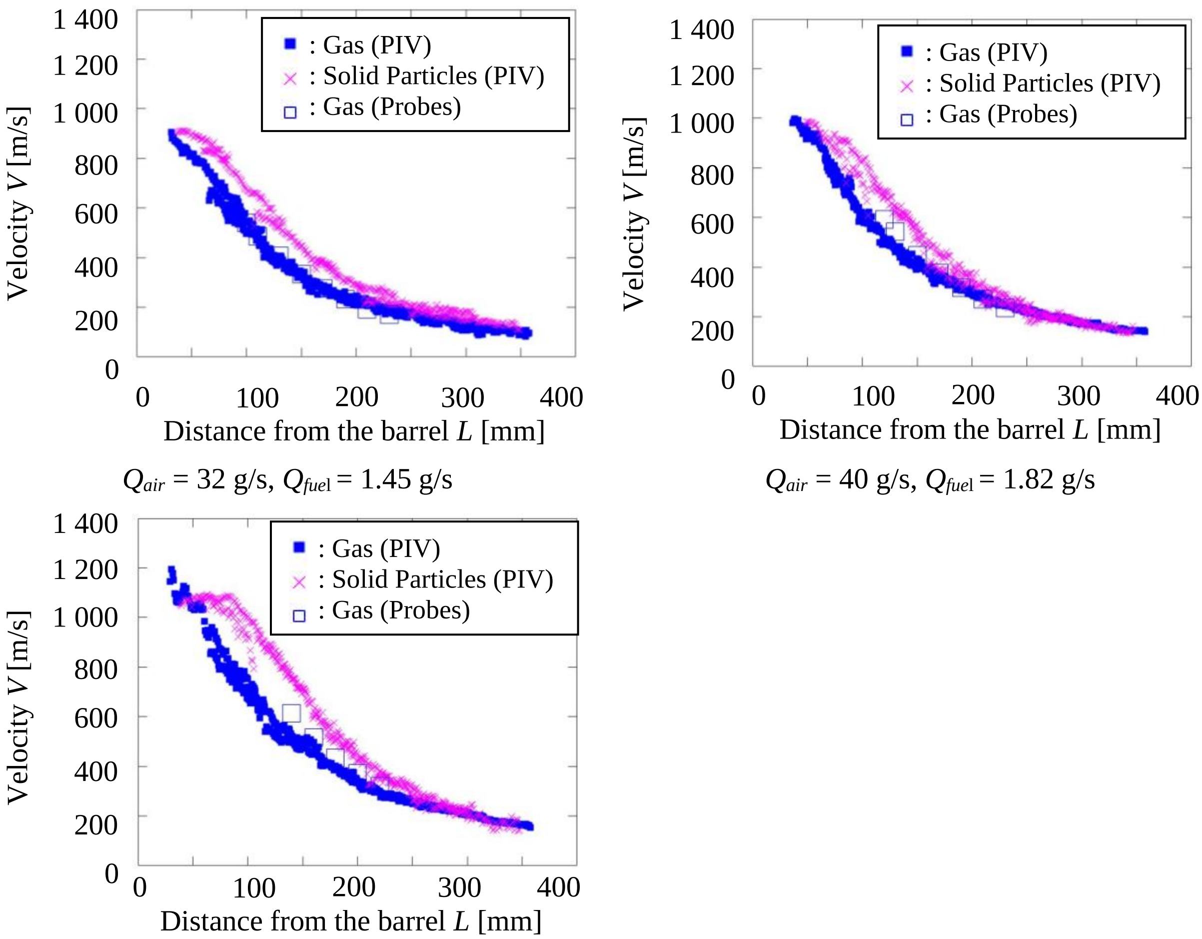

Q_{air} = 32 g/s, Q_{fuel} = 1.45 g/s

Q_{air} = 40 g/s, Q_{fuel} = 1.82 g/s

Q_{air} = 48 g/s, Q_{fuel} = 2.18 g/s

Fig. 5 Measurements of gas-solid two-phase jet by PIV, a temperature probe and pressure probes

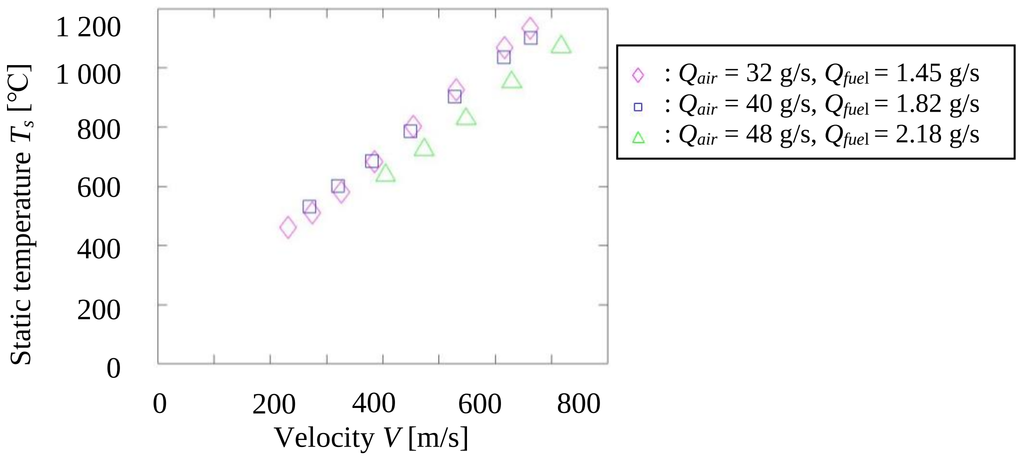

Fig.6 Velocity and static temperature of gas flow

diamond symbols are Q_{air} = 48 g/s, Q_{fuel} = 2.18 g/s. In all conditions, the static temperature is proportional to the velocity. In addition, the values of Q_{air} = 32 g/s, Q_{fuel} = 1.45 g/s, Q_{air} = 40 g/s, Q_{fuel} = 1.82 g/s were almost the same, and only Q_{air} = 48 g/s, Q_{fuel} = 2.18 g/s were hotter at the same speed than the other two conditions.

4. Conclusion

The following conclusions were obtained through the visualization and measurement of high-temperature high-speed solid-gas two-phase flow.
(1) The x-direction velocity component of the high-temperature high-speed solid-gas two-phase flow decreases as the distance from the barrel increases, and the z-direction velocity component has a component that moves away from the center of the flame.
(2) The validity of both PIV and probes measurements was shown, and the solid particle velocity was faster than the gas flow velocity except near the barrel.
(3) In a high-temperature, high-speed solid-gas two-phase flow, the static temperature and the velocity of solid particles are proportional.

References

[1] Balan, C. and Tabakoff, W., “Axial flow compressor performance deterioration”, *AlAA Paper*, 84-1208 (1984).

[2] Kuroda, S., Kawasaki, J., Watanabe, M. and Katanoda, H., “Warm spraying—a novel coating process based on high-velocity impact of solid particles”, *Sci. Technol. Adv. Mater.* 9 (2008), 033002.

[3] Suzuki, M. and Yamane, T., “Development of high-temperature high-velocity sand erosion apparatus”, *Proc. ASME Turbo Expo 2018*, GT2018-75044 (2018).

[4] Srivatsan, V.R. and Dolatabadi, A., “Simulation of Particle-Shock Interaction in a High Velocity Oxygen Fuel Process”, *Journal of Thermal Spray Technology*, vol. 15(4), December (2006), pp 481-487.